



# Removal of Surface Scale from Titanium Metal by Etching with HF-HNO<sub>3</sub> Mixed Acid

Mizuhata, Minoru  
Yamamoto, Shintaro  
Maki, Hideshi

---

(Citation)

Materials Transactions, 58(9):1280-1289

(Issue Date)

2017-09-01

(Resource Type)

journal article

(Version)

Version of Record

(Rights)

© 2017 The Japan Institute of Metals and Materials

(URL)

<https://hdl.handle.net/20.500.14094/90008356>



# Removal of Surface Scale from Titanium Metal by Etching with HF–HNO<sub>3</sub> Mixed Acid

Minoru Mizuhata<sup>1,\*1</sup>, Shintaro Yamamoto<sup>1,\*2</sup> and Hideshi Maki<sup>1,2</sup>

<sup>1</sup>Department of Chemical Science and Engineering, Graduate School of Engineering, Kobe University, Kobe 657–8501, Japan

<sup>2</sup>Center for Environmental Management, Kobe University, Kobe 657–8501, Japan

Etching of commercial pure titanium (CP-Ti) covered with metal oxide scale transferred to the surface from roller mills like those used for steel refining was investigated based on potentiodynamic polarization measurements and quantitative analysis of metal dissolved in HF or HF–HNO<sub>3</sub>. CP-Ti prepared by an industrial titanium supplier, titanium plate with scale (S-Ti), and annealed and pickled titanium (AP-Ti) were examined. The titanium substrate under the scale layer immediately dissolved in HF solution of concentration 1.0 mol·L<sup>−1</sup>. The etching behavior was examined in detail by electrochemical analysis in dilute HF. At HF concentrations less than 0.1 mol·L<sup>−1</sup>, the oxidized layer of S-Ti remained. X-ray photoelectron spectroscopy was used to identify the major components of the S-Ti surface, such as copper and iron impurities. In HF–HNO<sub>3</sub> solution, the scale was removed slowly, even at high HF concentrations. The amounts of dissolved titanium indicated that calcium on the titanium metal surface increased the etching rate, and the minimum apparent activation energies,  $\Delta E_a$ , of the etching reactions were observed at a concentration of 0.0316 mol·L<sup>−1</sup> HF aq. for S-Ti and AP-Ti because of the trade-off between the HF activity and ionic dissociation. Etching of CP-Ti began with dissolution of the passive layer of titanium; corrosion of S-Ti was the result of destruction of the titanium oxide layer by F<sup>−</sup> and dissolution of the pure titanium substrate. The etching behavior of S-Ti at high HF concentrations suggested that scale peeling by substrate etching is a promising method for efficient scale removal. The HNO<sub>3</sub> concentration had little effect on the anodic polarization curves of CP-Ti. This is attributed to the presence of a stable oxide layer on the titanium metal. We investigated the details of the S-Ti etching mechanism in HF–HNO<sub>3</sub> for efficient scale removal. [doi:10.2320/matertrans.M2017110]

(Received March 30, 2017; Accepted June 22, 2017; Published July 28, 2017)

**Keywords:** titanium, scale removal, apparent activation energy, potentiodynamic polarization, Tafel plot

## 1. Introduction

Titanium metal has high specific strength and biocompatibility, and superior etching resistance because of the passive film that spontaneously forms on the metal surface<sup>1,2</sup>. This thin oxide film forms easily in air and protects the inner active titanium metal from aggressive media. Titanium dioxide has a wide band gap, and titanium is therefore used in various applications, including photocatalysts, chemical sensors, and medical implants<sup>3–5</sup>. However, titanium metal and its alloys have disadvantages, e.g., metal-machining is difficult because of its thermal properties, and its production is expensive. Various new titanium-refining processes to replace the Kroll process have been developed<sup>6,7</sup> to reduce production costs or increase the quality of the titanium metal produced. Suzuki *et al.*<sup>8</sup> developed the Ono–Suzuki process, which involves calciothermic reduction and electrolysis of CaO in the molten salt. The Fray–Farthing–Chen Cambridge process, in which oxygen is removed from metal oxides by electrolysis in CaCl<sub>2</sub> molten salt, has been used for the reduction of various metals, including titanium<sup>9,10</sup>. The costs of titanium metal production can also be reduced by using roller milling, which is used in steel refining<sup>11</sup>. However, this method causes a new problem in titanium metal production.

Figure 1 shows the formation of titanium metal by hot rolling and cold rolling. A black metal oxide, which is referred to as scale, is formed on the titanium metal surface during hot rolling<sup>12</sup>. This scale contains impurities derived from contact with the milling roller, inhibits metal surface treatment, and damages the appearance of the metal, there-

fore the scale is removed by pickling. Fluoride solutions such as HF aq. are well known as corrosive media for titanium oxide, however it is difficult to remove scale by its dissolution in HF aq. Scale removal by fluorides proceeds via scale separation rather than dissolution. The HF aq. penetrates the crevices in a non-uniform scale and corrodes the titanium substrate under the scale, as shown in Fig. 1, causing peeling of the scale. Scale can be removed from large quantities of titanium substrates by etching with highly concentrated HF aq., however this is inefficient. The addition of an oxidizing acid such as HNO<sub>3</sub> aq. to HF aq. in practical pickling processes enables mild etching of the scale, therefore investigation of the details of the mechanism of scale removal from titanium metal by etching in HF–HNO<sub>3</sub> is required. The aim of this study was clarification of the titanium-etching mechanism in fluoride-containing acid solutions, and identification of the best etching conditions, to minimize substrate damage.

The etching behaviors of titanium metal and its alloys in acids containing various corrosive species have been reported. Nady *et al.*<sup>13</sup> investigated the effects of chloride and sulfide by examining the electrochemical properties of Cu, Cu–10Al–10Ni, carbon steel, and commercial pure titanium (CP-Ti) in 3.5% sodium chloride containing sulfide ions. They found that the etching resistance of CP-Ti was higher than those of the other metals in chloride–sulfide media. Shankar *et al.*<sup>14</sup> investigated the etching resistance of thermally oxidized CP-Ti in boiling HNO<sub>3</sub>. Wang *et al.*<sup>15,16</sup> determined the pH-related critical fluoride concentration for CP-Ti etching in fluoride solution based on electrochemical parameters. The polarization curves for titanium etching in HF–HNO<sub>3</sub> have also been reported<sup>17</sup>. However, further investigation of titanium metal etching by direct pickling of titanium scale is needed. In this work, the etching behaviors

\*1Corresponding author, E-mail: mizuhata@kobe-u.ac.jp

\*2Graduate Student, Kobe University

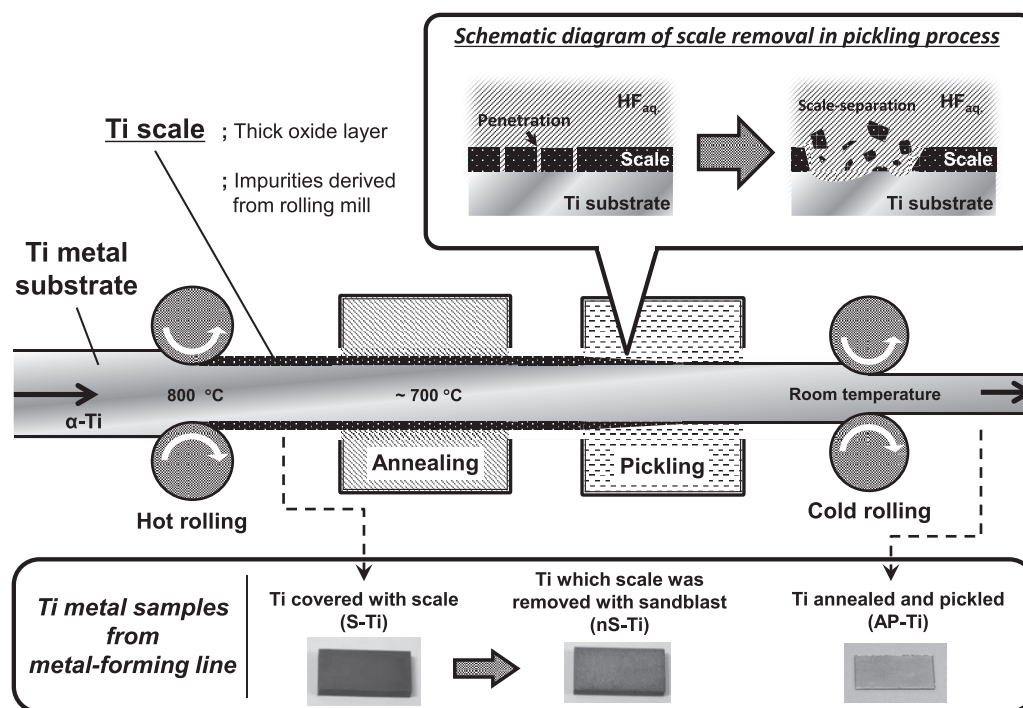


Fig. 1 Ti metal forming process.

of titanium metal covered with scale (S-Ti) and CP-Ti were investigated in pure HF aq. HNO<sub>3</sub> aq. was added as an oxidizing acid to HF aq. to adjust the substrate stability and F<sup>-</sup> activity. In addition to this, corrosion behaviors of titanium metal annealed and etched with HF (AP-Ti) is investigated to reveal the effects of annealing and pickling in practical Ti production line on titanium metal surface. Etching of S-Ti in the mixed acid was also performed. The etching behaviors of these metals were analyzed in terms of the amount of dissolved titanium ions. Electrochemical measurements were performed on CP-Ti. The ability of each acid to remove titanium scale was also evaluated by surface analysis. We propose a mechanism for etching titanium metal with scale on its surface using an acid solution containing fluoride.

## 2. Experimental

### 2.1 Preparation of corrosive solution

HF aq. and HF-HNO<sub>3</sub> mixed aqueous solutions were used as the electrolytes for electrochemical measurements and etching solutions in etching tests. Each acid was diluted with deionized water; the acid concentrations used in the measurements are given below.

### 2.2 Etching tests for CP-Ti and S-Ti

An S-Ti sample (gifted by Kobe Steel, Ltd.) and commercial grade 2 titanium sheet (CP-Ti; Japan Metal Service Co., Ltd., Ti-08-0001) were used as etching samples. The S-Ti dimensions were width × length × height = 10 × 20 × 4 mm<sup>3</sup>, and the vertical side surface was covered with scale. The thickness of the scale layer was measured ca. 2.2 ± 0.3 μm by the cross sectional SEM observation. The CP-Ti dimensions were width × length × height = 16 × 20 × 0.1 mm<sup>3</sup>. The chemical compositions of S-Ti substrate and

CP-Ti are almost identical each other. These samples were ultrasonically cleaned with acetone before the etching tests. The etching solutions were  $x$  mol·L<sup>-1</sup> HF +  $y$  mol·L<sup>-1</sup> HNO<sub>3</sub> in deionized water (in HF solution,  $x = 0.01$ – $0.1$  and  $y = 0$ ; in HF-HNO<sub>3</sub> solution,  $x = 0.01, 0.1$ , and  $1$ , and  $y = 0.0078$ – $0.09, 0.078$ – $0.9$ , and  $0.78$ – $9$ , respectively). The titanium samples were hung on threads and immersed in the etching solution (20 mL). The immersion time was 10–180 min for low acid concentrations (i.e., 0.01–0.1 mol·L<sup>-1</sup> HF aq.; 0.01 mol·L<sup>-1</sup> HF aq./0–0.09 mol·L<sup>-1</sup> HNO<sub>3</sub> aq.; and 0.1 mol·L<sup>-1</sup> HF aq./0–0.9 mol·L<sup>-1</sup> HNO<sub>3</sub> aq.), and 1–18 min for high acid concentrations (i.e., 0.1–1 mol·L<sup>-1</sup> HF aq.; 1 mol·L<sup>-1</sup> HF aq./0–9 mol·L<sup>-1</sup> HNO<sub>3</sub> aq.) The samples were removed from the etching solutions after a predetermined time and the amounts of titanium ions dissolved in the etching solutions were determined using inductively coupled plasma-atomic emission spectroscopy (ICP-AES; HORIBA, Ltd., ULTIMA2000). Ultraviolet-visible (UV-vis) spectroscopy (JASCO International Co., Ltd., V-7200) was used to investigate the titanium ionic state in the etching solution. The apparent activation energies at 30–50 °C were determined from Arrhenius plots.

### 2.3 Etching tests for AP-Ti

For comparison, AP-Ti sample (gifted by Kobe Steel, Ltd.) was partly corroded under the acid conditions described above. The AP-Ti dimension was width × length × height = 10 × 20 × 1 mm<sup>3</sup>. The sample was ultrasonically cleaned with acetone before the etching tests. The etching solutions were 0.01–0.1 mol·L<sup>-1</sup> HF in deionized water. The titanium specimens were hung using thread which is made of polyethylene and immersed in the etching solution (20 mL). The hydrogen gas bubble generation did not confirm during the etching process, thus the influence of the

convection of the solution by hydrogen gas bubble can be disregarded. After etching for 10–180 min, the samples were removed from the etching solutions and the amounts of dissolved titanium ions in the etching solutions were determined using ICP-AES. The apparent activation energies at 30–50°C were determined from Arrhenius plots.

## 2.4 Surface characterization

The surface morphology was examined and the scale-etching progress was monitored using field-emission scanning electron microscopy (FE-SEM; JEOL Co., Ltd., JEM6335F) and energy dispersive X-ray spectroscopy (EDX; JEOL Co., Ltd., JED2200) at an accelerating voltage of 15 kV. The surface compositions and chemical states were investigated by X-ray photoelectron spectroscopy (XPS; JEOL Co., Ltd., JPS9010MC) using a standard Al K $\alpha$  radiation source. Binding energies were corrected using Au, Ag and Cu. The Ti 2p, Fe 2p, and Cu 2p XP spectra aligned to the Au peak at 84.0 eV were recorded.

## 2.5 Electrochemical measurements

All electrochemical measurements were performed in a three-electrode cell. The electrochemical cell consisted of a platinum sheet as a counter electrode, saturated Ag|AgCl reference electrode connected to the cell via a KCl salt bridge with a Luggin capillary and the specimen, and CP-Ti as the working electrode. All electrode potentials were measured versus Ag|AgCl. The working electrode was masked using adhesive tape, leaving a 2.0 cm<sup>2</sup> exposed area. Its surface was mechanically polished with 1  $\mu$ m diamond paste (BAS Co., Ltd., 012621) and 0.05  $\mu$ m alumina paste (BAS Co., Ltd., 012620), and then ultrasonically cleaned with acetone. The electrolyte solutions were  $x$  mol·L<sup>-1</sup> HF +  $y$  mol·L<sup>-1</sup> HNO<sub>3</sub> in deionized water (in HF solution,  $x$  = 0.01–0.1 and  $y$  = 0; in HF–HNO<sub>3</sub> solution,  $x$  = 0.01 and  $y$  = 0.0078–0.09). Open-circuit potential (OCP) measurements were performed for at least 30 min, and then potentiodynamic polarization tests were performed from –0.3 V versus determined OCP to 0.6 V in HF solution, and from –0.2 mV versus determined OCP to 0.6 V in HF–HNO<sub>3</sub> solution at a scanning rate of 0.5 mV s<sup>-1</sup>. The electrolyte solutions were deaerated by nitrogen gas bubbling for at least 15 min before all electrochemical measurements, and a nitrogen gas tube was set above the solution during the measurements. All measurements were performed without stirring at 30°C.

## 3. Results and Discussion

### 3.1 Dependence of scale-removed progress on acid concentration

The differences between the S-Ti sample, which had been masked with acid-proofed tape and corroded in 1 mol·L<sup>-1</sup> HF aq. for 6 min, and CP-Ti were investigated using SEM-EDX. Figure A1(a) shows a photograph of the masked S-Ti after etching for 6 min in 1 mol·L<sup>-1</sup> HF aq.; Figure A1(b) shows SEM images of S-Ti and TiO<sub>2</sub> powder on a carbon sheet as a reference sample, and the EDX line profiles of titanium and oxygen. Figure A1(b) confirms that the surface scale had non-uniform titanium and oxygen intensities, and the substrate surface had a uniformly high titanium intensity

and low oxygen intensity. SEM images of S-Ti samples which were corroded with acids of various concentrations and EDX line profiles of titanium and oxygen are shown in Fig. 2. All the images in Fig. 2 show TiO<sub>2</sub> powder on a carbon sheet on the left as a standard sample, and the EDX intensities of titanium and oxygen were normalized for comparison. When all SEM-EDX spectra were measured, the carbon sheets which puts the TiO<sub>2</sub> powder as a standard sample were also measured at the same time as shown in each SEM image of Fig. 2. Therefore, a quantitative comparison between Ti and O of the S-Ti sample using SEM-EDX will be possible. In addition, the amount of dissolved titanium in each etching solution is shown in Fig. 2. Figure 2(a) and (c) show non-uniform titanium intensities and a relatively high oxygen peak. Figure 2(b) and (d) show constantly high titanium peaks and low oxygen peaks. These results indicate that part of the thick oxide layer remained on the samples in Fig. 2 (a) and (c). This suggests that scale etching was insufficient at HF concentrations of 0.1 mol·L<sup>-1</sup> or less. It is worth noting that the scale-peeled sample obtained by etching for 18 min in 1 mol·L<sup>-1</sup> HF aq./9 mol·L<sup>-1</sup> HNO<sub>3</sub> aq. had a satisfactory surface, however gave a lower amount of dissolved titanium than did the S-Ti sample after etching for 180 min in 0.1 mol·L<sup>-1</sup> HF aq., as shown in Fig. 2. The chemical compositions of S-Ti and AP-Ti were determined using XPS before the etching tests (Fig. A2). Iron and copper impurities were observed on S-Ti, which was not corroded; these were derived from contact with the equipment during hot rolling. The calcium signal from AP-Ti was clearer than in the cases of S-Ti, although there was no scale on AP-Ti. The calcium comes from CaF<sub>2</sub>, which was formed during washing with industrial water after HF etching because fluoride remaining on the titanium surface can react with calcium cations in industrial water. After etching, the S-Ti samples were examined using XPS to investigate the presence of impurities in the titanium scale and degree of impurity removal by etching (Figs. A3 and A4). Iron was removed by a low concentration of HF aq., however copper still remained. In contrast, iron and copper were both removed in HF–HNO<sub>3</sub> solution. This confirms that the addition of HNO<sub>3</sub> to HF aq. enables efficient copper removal.

### 3.2 Dependence of the amount of dissolved titanium on added HNO<sub>3</sub> concentration

When the HF concentration is over 0.3 mol·L<sup>-1</sup>, the noticeable H<sub>2</sub> gas bubble generation could not be confirmed. It can be estimated that the H<sub>2</sub> was dissolved into electrolyte or absorbed into titanium alloys. On the other hand, when the HF concentration is over 0.3 mol·L<sup>-1</sup>, the H<sub>2</sub> gas bubble generation was confirmed, and it can be estimated that this H<sub>2</sub> gas bubble generation hardly affects the reliability of data, because there were good reproducibilities in the following experimental data. The amounts of dissolved titanium from S-Ti in HF aq. solution of concentration 0.01–0.1 mol·L<sup>-1</sup> are shown in Fig. 3(a). It is estimated that a series of the etching process is almost identical, therefore the apparent corrosion depth  $D$  of S-Ti was calculated from the amount of dissolved titanium  $M_T$ ;

$$D = mM_{\text{Ti}}/d \quad (1)$$



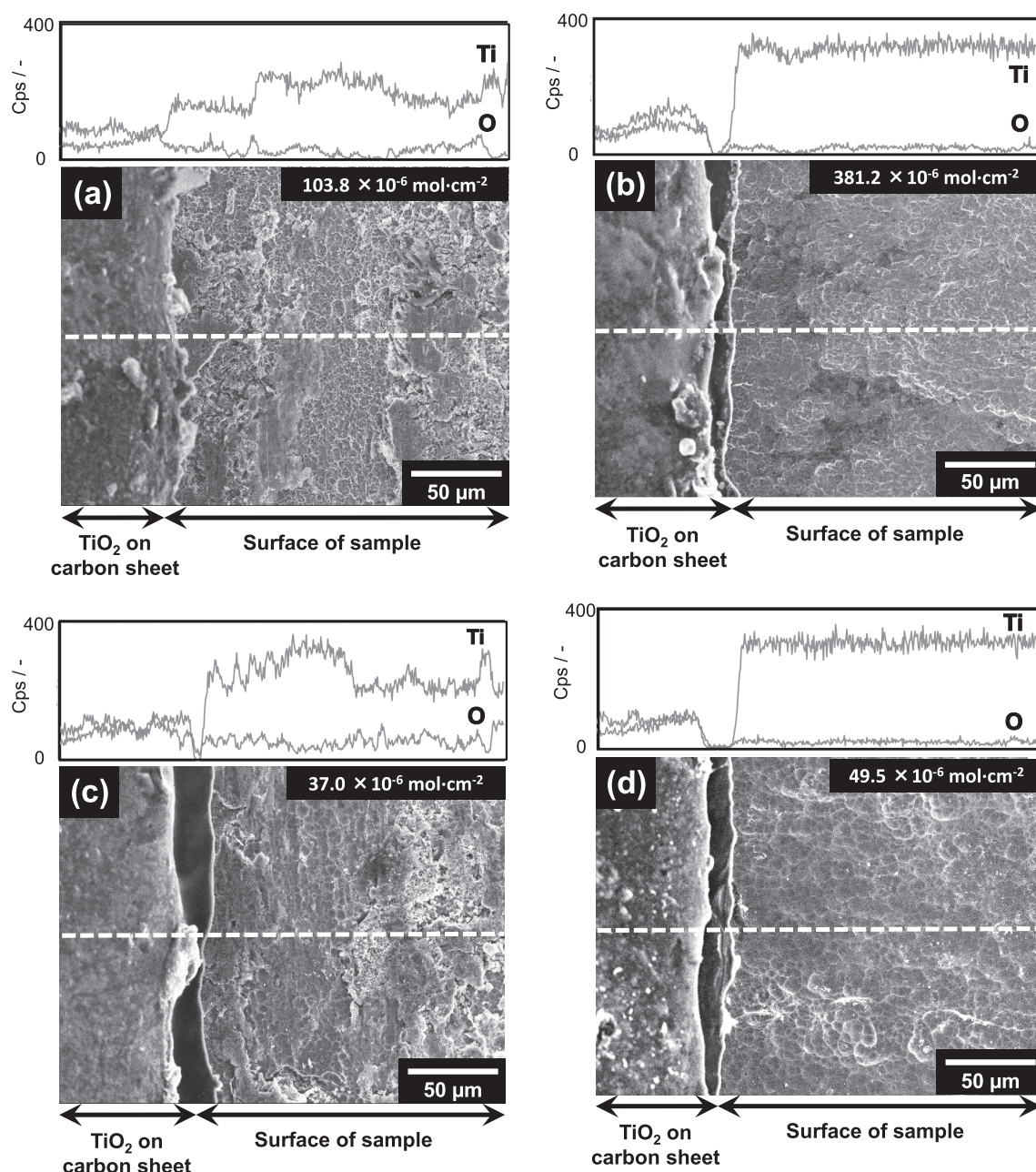
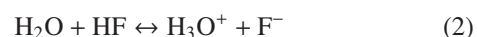


Fig. 2 SEM images of S-Ti and EDX line profiles of Ti and O in (a) 0.1 mol·L<sup>-1</sup> HF aq. after 180 min, (b) 1 mol·L<sup>-1</sup> HF aq. after 180 min, (c) 0.1 mol·L<sup>-1</sup> HF aq./0.9 mol·L<sup>-1</sup> HNO<sub>3</sub> aq. after 180 min, (d) 1 mol·L<sup>-1</sup> HF aq./9 mol·L<sup>-1</sup> HNO<sub>3</sub> aq. after 18 min (dotted line is EDX measured area).

where  $m$  is the atomic weight of titanium and  $d$  is the density of S-Ti. The amounts of dissolved titanium from S-Ti increased with increasing HF concentration because of the increased number of corrosive species, i.e.,  $F^-$  and  $H^+$ . As mentioned below, HF aq. in the concentration range 0.01–0.1 mol·L<sup>-1</sup> did not achieve scale removal. At higher HF aq. concentrations, the amount of titanium dissolved from S-Ti was higher, even at shorter immersion times, as shown in Fig. 3(b). A black supernatant from the separated scale was observed in the etching solution during the etching tests; this supports the SEM-EDX results, which showed that scale was adequately removed at a concentration of 1 mol·L<sup>-1</sup>. However, use of 1 mol·L<sup>-1</sup> HF is insufficient for scale removal because dissolution of the titanium substrate is too high. The optimum acid conditions were determined by in-

vestigating the use of HF–HNO<sub>3</sub> solution.

The amounts of dissolved titanium from S-Ti in HF–HNO<sub>3</sub> solution consisting of 0.01 mol·L<sup>-1</sup> HF aq./0–0.09 mol·L<sup>-1</sup> HNO<sub>3</sub> aq. are shown in Fig. 3(c); the figure shows that the amount of dissolved titanium from S-Ti was the lowest in 0.01 mol·L<sup>-1</sup> HF aq./0.0078 mol·L<sup>-1</sup> HNO<sub>3</sub> aq. This inhibitory effect of corrosion by HNO<sub>3</sub> addition arises because S-Ti is affected more strongly by the  $F^-$  activity, which depends on the degree of acid dissociation;  $F^-$  destroys the titanium oxide layer. The acid dissociation equilibrium is represented by



The S-Ti surface is covered with metal oxides, including scale, therefore the  $F^-$  activity is the dominant factor in S-Ti

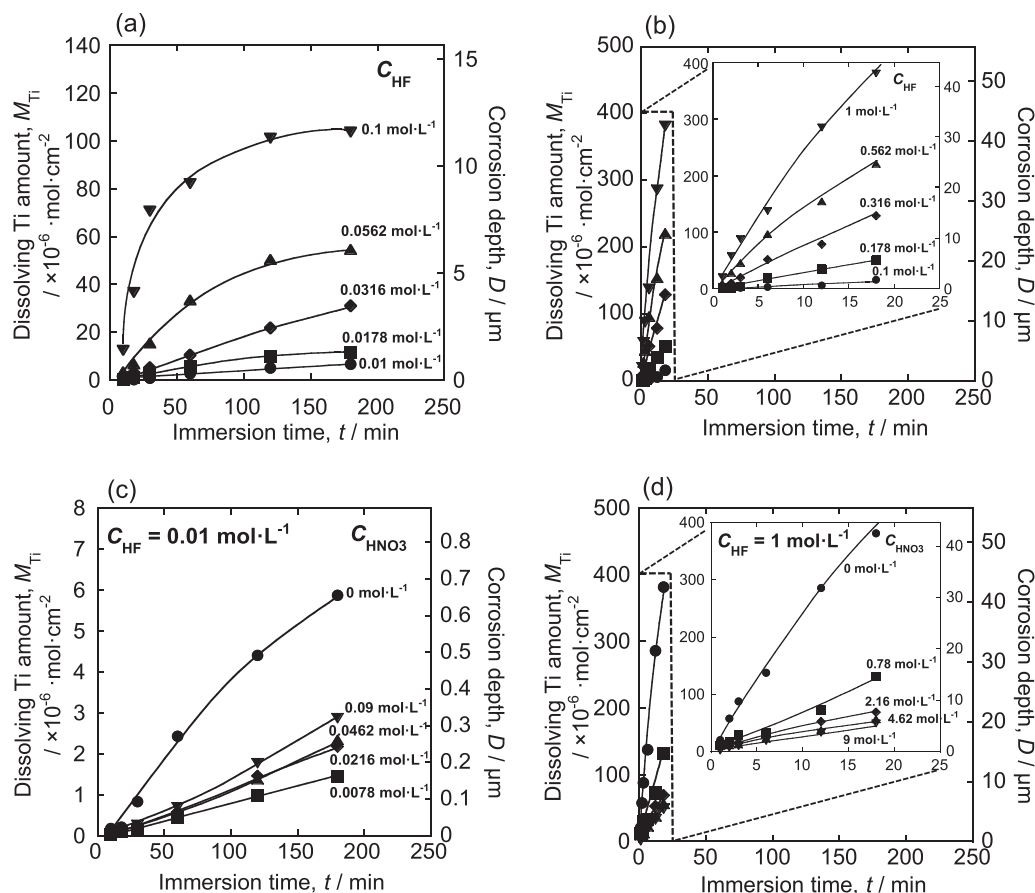
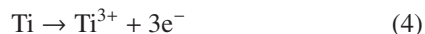


Fig. 3 Dissolved Ti amount in (a) 0.01–0.1 mol·L<sup>-1</sup> HF aq. with S-Ti, (b) 0.1–1 mol·L<sup>-1</sup> HF aq. with S-Ti, (c) 0.01 mol·L<sup>-1</sup> HF aq./0–0.09 mol·L<sup>-1</sup> HNO<sub>3</sub> aq. with S-Ti, (d) 1 mol·L<sup>-1</sup> HF aq./0–9 mol·L<sup>-1</sup> HNO<sub>3</sub> aq. with S-Ti.

etching rather than the H<sup>+</sup> activity. Furthermore, the increase in the amount of dissolved titanium with increasing HNO<sub>3</sub> concentration (Fig. 3(c)) suggests that the increase in titanium substrate etching under the scale is a result of increased H<sup>+</sup> activity rather than F<sup>-</sup> etching. This means that the titanium-etching rate depends on F<sup>-</sup>, which destroys titanium oxide, and H<sup>+</sup> which is involved in etching the exposed titanium subsate.



The hydrogen reduction reaction is represented by<sup>18)</sup>



and



or



The transition spectra of some TiF<sub>6</sub><sup>3-</sup> salts show distinct splittings<sup>19)</sup>; the presence of Ti<sup>3+</sup> in HF aq. after S-Ti etching, confirmed using UV-vis spectroscopy (Fig. A5), suggests that these equations apply. In the case of a high-concentration HF–HNO<sub>3</sub> solution (1 mol·L<sup>-1</sup> HF aq./0.78 mol·L<sup>-1</sup> HNO<sub>3</sub> aq.), the amount of dissolved titanium increased consistently with increasing HNO<sub>3</sub> concentration,

as shown in Fig. 3(d). This indicates that there is an upper limit to the etching rate by H<sup>+</sup>, therefore the F<sup>-</sup> activity is the dominant factor at high HF–HNO<sub>3</sub> concentrations. Similar scale separation was confirmed for S-Ti etching in high-concentration HF solution (Fig. 3(b)). These scale separation phenomena indicates that the dissolution of the titanium substrate under scale. Ti substrate is etched preferentially by acidic solution infiltrating the gap of scale, and scale lost the substrate is peeled off. As mentioned above, the scale-peeled sample obtained by etching for 18 min in 1 mol·L<sup>-1</sup> HF aq./9 mol·L<sup>-1</sup> HNO<sub>3</sub> aq. had a satisfactory surface with a relatively low amount of dissolved titanium. This result can be attributed to multiple etching processes by F<sup>-</sup> and H<sup>+</sup>. Substrate etching by decreasing the pH is therefore a better method for removing scale quickly and efficiently.

### 3.3 Influence of the impurities on titanium metal on the amount of dissolved titanium

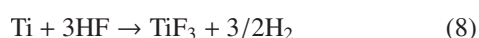
The etching behaviors of S-Ti and AP-Ti were compared based on the amounts of dissolved titanium ions in the HF etching solutions to reveal the influence of impurities on titanium metal on the amount of dissolved titanium. Typical graphs are shown in Fig. 4. AP-Ti gave the lowest amount of dissolved titanium in the initial stage (Fig. 4(a)). This indicates that the calcium on AP-Ti increased the etching resistance of AP-Ti. The amount of dissolved titanium from AP-Ti overtook those from the others with time; this can be

attributed to the consumption of corrosive species formed by dissolution of impurities on S-Ti. Figure 4(b) shows that at low HF concentrations, S-Ti gave the lowest amount of dissolved titanium, and 0.0178 mol·L<sup>-1</sup> HF aq. was unable to destroy the scale on S-Ti.

### 3.4 Dependence of the apparent activation energy on acid concentration

The apparent activation energies,  $\Delta E_a$ , for etching S-Ti and AP-Ti in 0.01–0.1 mol·L<sup>-1</sup> HF aq. were obtained from Arrhenius plots. We did not have a large enough number of AP-Ti samples, therefore the amount of dissolved titanium after etching for 10 min was regarded as the initial titanium-etching rate,  $r$ , and we assumed the following.

- (1) The titanium activity is constant.
- (2) The titanium-etching reaction in HF aq. is expressed by



$$r = kC_{\text{HFi}} = 3C_{\text{Ti}}/st \quad (9)$$

where  $k$  is the apparent reaction rate constant,  $C_{\text{HFi}}$  is the initial HF concentration,  $C_{\text{Ti}}$  is the dissolved titanium concentration,  $s$  is the total etching area of the titanium sample, and  $t$  is the immersion time. The Arrhenius plots of the amounts of dissolved titanium and obtained  $\Delta E_a$  values are shown in Fig. A6 and Fig. 5(a), respectively. The  $\Delta E_a$  values for all the samples were lowest in 0.0316 mol·L<sup>-1</sup> HF aq. This can be attributed to changes in the degree of dissociation of HF with changes in HF concentration. The dissociation degree( $\alpha$ ) in Fig. 5(a) can be calculated, assuming that the following equation holds:

$$\alpha = \frac{-K_a + \sqrt{K_a^2 + 4K_a(C_{\text{H}} + C_{\text{HF}})}}{2(C_{\text{H}} + C_{\text{HF}})} \quad (10)$$

where  $K_a$  is the dissociation constant of HF as follows;

$$K_a = C_{\text{H}}C_{\text{F}^-}/C_{\text{HF}} = 6.76 \times 10^{-4} \text{ mol} \cdot \text{L}^{-1} \quad (11)^{(20)}$$

The largest change in  $\Delta E_a$  with changes in HF concentration

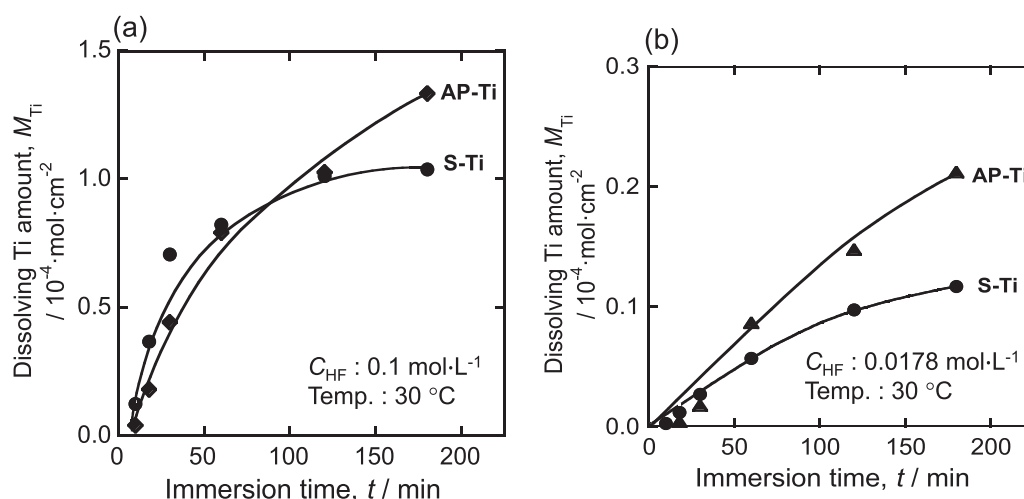


Fig. 4 Dissolved Ti amount with S-Ti and AP-Ti in HF system, (a) 0.1 mol·L<sup>-1</sup> HF aq., (b) 0.0178 mol·L<sup>-1</sup> HF aq.

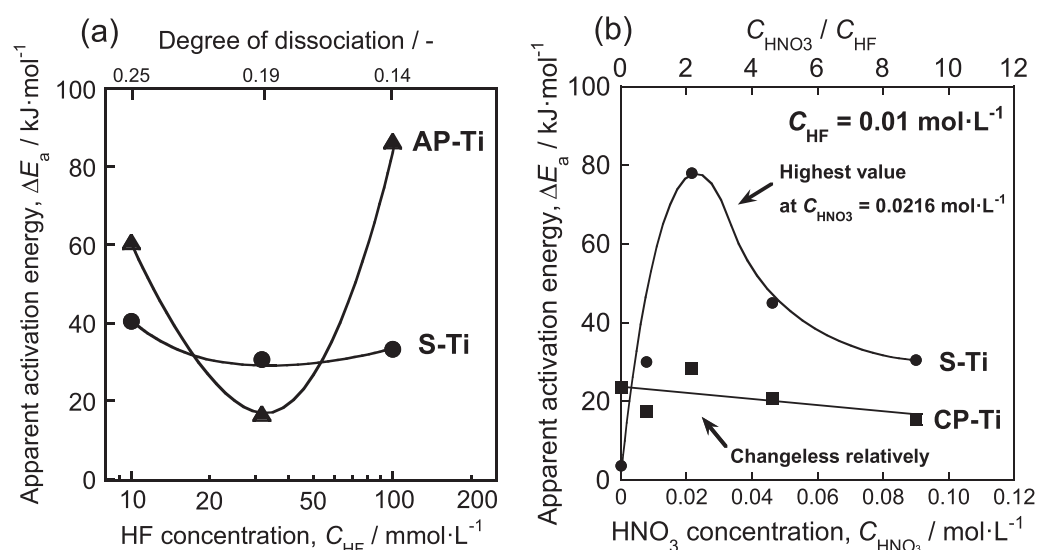


Fig. 5 Apparent activation energies of (a) S-Ti and AP-Ti in 0.01–0.1 mol·L<sup>-1</sup> HF aq., (b) S-Ti and CP-Ti in 0.01 mol·L<sup>-1</sup> HF aq./0–0.09 mol·L<sup>-1</sup> HNO<sub>3</sub> aq. at a temperature range of 30–50°C.

was observed for AP-Ti because of the contribution of calcium on the AP-Ti surface. The values for CP-Ti and S-Ti in  $0.01 \text{ mol}\cdot\text{L}^{-1}$  HF aq./ $0\text{--}0.09 \text{ mol}\cdot\text{L}^{-1}$  HNO<sub>3</sub> aq. were calculated from Arrhenius plots obtained from the initial titanium-etching rate. The initial etching rate was determined from the slopes of fitting curves extrapolated to a dissolved titanium amount of 0, as shown in Fig. 6, and the initial etching rates were shown in Fig. A7. The assumptions for the determination of  $\Delta E_a$  are as follows.

1. The titanium activity is constant.
2. The initial titanium-etching rate can be used as the apparent reaction rate constant,  $k$ .
3. The initial titanium-etching rate can be calculated from the extrapolated fitting curve for the graph of dissolved titanium amount versus immersion time.

Arrhenius plots at  $30\text{--}50^\circ\text{C}$  were prepared (Fig. A8). The

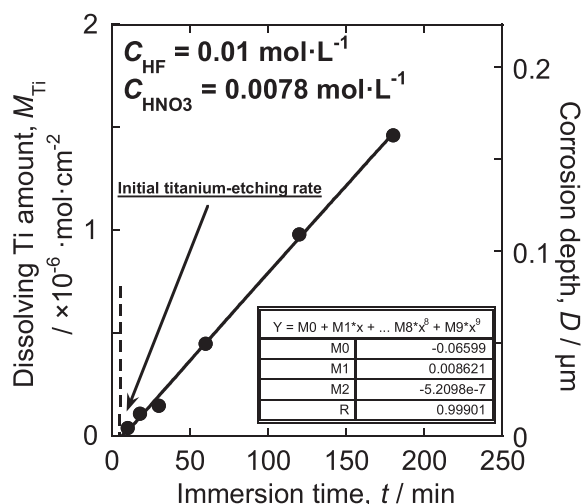


Fig. 6 Correlation between the dissolving Ti amount and the immersion time. The initial etching rate was determined from the slopes of fitting curves extrapolated to a dissolved titanium amount of 0.

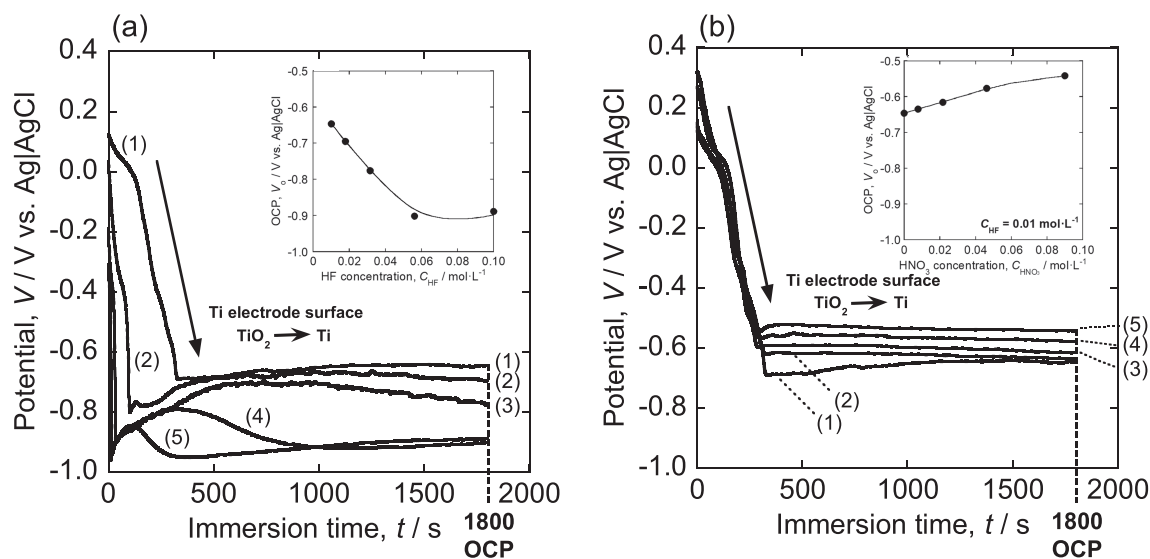


Fig. 7 OCP measurements for CP-Ti in (a) HF system and (b) HF-HNO<sub>3</sub> system. Inset figures show the determined OCP. (a): (1)  $0.01 \text{ mol}\cdot\text{L}^{-1}$  HF, (2)  $0.0178 \text{ mol}\cdot\text{L}^{-1}$  HF, (3)  $0.0316 \text{ mol}\cdot\text{L}^{-1}$  HF, (4)  $0.0562 \text{ mol}\cdot\text{L}^{-1}$  HF, (5)  $0.10 \text{ mol}\cdot\text{L}^{-1}$  HF; (b)  $0.01 \text{ mol}\cdot\text{L}^{-1}$  HF, (2)  $0.01 \text{ mol}\cdot\text{L}^{-1}$  HF +  $0.0078 \text{ mol}\cdot\text{L}^{-1}$  HNO<sub>3</sub>, (3)  $0.01 \text{ mol}\cdot\text{L}^{-1}$  HF +  $0.0216 \text{ mol}\cdot\text{L}^{-1}$  HNO<sub>3</sub>, (4)  $0.01 \text{ mol}\cdot\text{L}^{-1}$  HF +  $0.0462 \text{ mol}\cdot\text{L}^{-1}$  HNO<sub>3</sub>, (5)  $0.01 \text{ mol}\cdot\text{L}^{-1}$  HF +  $0.0900 \text{ mol}\cdot\text{L}^{-1}$  HNO<sub>3</sub>.

$\Delta E_a$  values obtained from the slopes of the Arrhenius plots are shown in Fig. 5(b). The  $\Delta E_a$  of CP-Ti decreased slightly with increasing added HNO<sub>3</sub> concentration, whereas S-Ti had a maximum  $\Delta E_a$  in  $0.01 \text{ mol}\cdot\text{L}^{-1}$  HF aq./ $0.0216 \text{ mol}\cdot\text{L}^{-1}$  HNO<sub>3</sub> aq. This difference again suggests different degrees of contribution by F<sup>-</sup> and H<sup>+</sup> to etching depending on the titanium surface condition. The aggressiveness of the HF solution toward S-Ti can therefore be reduced by HNO<sub>3</sub> addition to the HF solution; this is useful for optimization of the degree of etching of S-Ti. In conclusion, titanium dissolution can occur through multiple reaction processes, e.g., passive layer destruction by fluoride ions and oxidation of the active substrate. Scale etching by substrate etching with HF-HNO<sub>3</sub> is a promising method for efficient scale removal.

### 3.5 Determination of Open-circuit potential

Figure 7(a) and (b) shows the results of OCP measurements with CP-Ti working electrodes. The rapid decreases in the potentials in the initial stage indicate a transformation of the titanium surface state, i.e., from TiO<sub>2</sub> to titanium. Moreover, the potential behaviors in HF-HNO<sub>3</sub> solution were flat compared with that in HF solution. The HF activity in the HF solution will be higher than that in the HF-HNO<sub>3</sub> solution. Thus it can be considered that almost all TiO<sub>2</sub> have been oxidized to Ti immediately after immersion into the HF solution. On the other hand, the TiO<sub>2</sub> will still remain after immersion into the HF-HNO<sub>3</sub> solution, therefore the mixed potential of TiO<sub>2</sub> and Ti is observed for the HF-HNO<sub>3</sub> solution, and as a result, the electrical potential behavior becomes flat. In this study, reasonably stable OCPs were obtained after 30 min; the determined OCPs are shown in the inset in Fig. 7. The OCP decreased with increasing HF concentration, showing an increase in the anodic current density, i.e., an increase in the titanium-etching rate. In contrast, in HF-HNO<sub>3</sub> solution, the OCP increased with increasing HNO<sub>3</sub> concentration. This shows an increase in the cathodic current density, i.e., an increase in the HER rate.



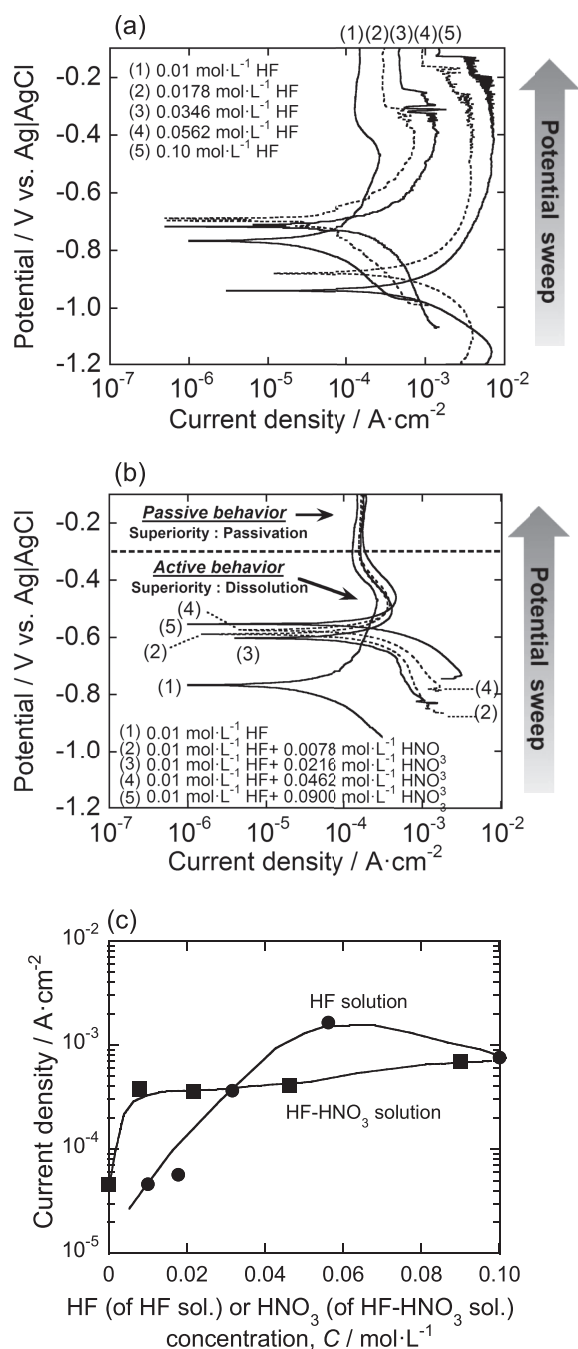


Fig. 8 Potentiodynamic polarization test for CP-Ti in (a) HF system, (b) HF-HNO<sub>3</sub> system, and (c) the corrosion current densities,  $I_{\text{corr}}$ , which were calculated from the polarization curves.

### 3.6 Titanium corrosion behaviors with potentiodynamic polarization test

Potentiodynamic polarization measurements were performed at the above OCPs, which were used as indication potentials; the results are shown in Fig. 8(a) and (b). The obtained polarization curves showed behavior typical of valve metals, i.e., they showed active dissolution behavior and passivation behavior in the anodic curve. There are some disturbances of current densities in (2)–(5) in Fig. 8(a) at the potential range from  $-0.14$  V to  $-0.4$  V; it can be attributed to the adhesion of H<sub>2</sub> bubbles on the Ti electrode surface. In HF solution, the anodic and cathodic current density both increased with increasing HF concentration, whereas in HF–

HNO<sub>3</sub> solution, the anodic current density showed little change. In particular, passivation current density behaviors (above  $-0.3$  V in Fig. 8(b)) appeared at similar potential ranges for various HNO<sub>3</sub> concentrations. These results indicate that fluoride promotes both the titanium-etching rate and the HER rate, however protons only significantly influence the HER rate<sup>21</sup>). This difference between the effects of fluoride and protons is caused by the presence of a stable oxide layer on the CP-Ti surface. The corrosion rates,  $I_{\text{corr}}$ , which were calculated from the polarization curves were shown in Fig. 8(c). The  $I_{\text{corr}}$  for HF solution was tend to increase with HF concentration, and it can be attributed to an increase of the Ti corrosion rate by fluoride. On the other hand, in the case of HF-HNO<sub>3</sub> solution, there was relatively little change at each electrochemical parameter, especially in passive region. These results indicate that HNO<sub>3</sub> concentration (that is, H<sup>+</sup> activity) in this work's range has little influence to Ti oxide layer.

In conclusion, the anodic and cathodic behaviors both depend significantly on the HF concentration, because of the increases in F<sup>−</sup> and H<sup>+</sup> activities, however HNO<sub>3</sub> added at the concentrations used in this work has little influence on the anodic behaviors. This behavior indicates that protons do not eliminate the titanium oxide layer. Fluoride in an acid is therefore essential for removal of the scale on a titanium substrate.

### 4. Conclusions

In this study, we analyzed the titanium corrosion behaviors in HF containing acids by quantitative determination of the amount of dissolved titanium, surface analysis of titanium metal, and electrochemical measurements. Then we revealed the corrosion mechanism for etching titanium metal with scale. SEM-EDX showed that scale was not completely removed at HF concentrations of 0.1 mol·L<sup>-1</sup> or less. XPS showed HF aq. removed iron on S-Ti, but did not completely remove copper on S-Ti. The addition of HNO<sub>3</sub> to HF aq. promoted copper removal. Moreover, the amounts of dissolved titanium from AP-Ti was low due to calcium on the titanium metal surface adhered at industrial water washing after pickling. The amount of dissolved titanium from S-Ti increased with HF concentration. The dependence of the amounts of dissolved titanium from S-Ti in HF-HNO<sub>3</sub> solution on added HNO<sub>3</sub> concentration can be attributed that the contribution of activities of F<sup>−</sup> and H<sup>+</sup>. The  $\Delta E_a$  values of S-Ti and AP-Ti were lowest at 0.0316 mol·L<sup>-1</sup> HF aq.; this is attributed to a change in the degree of HF dissociation. The  $\Delta E_a$  of S-Ti in HF-HNO<sub>3</sub> solution was maximum at 0.01 mol·L<sup>-1</sup> HF aq./0.0216 mol·L<sup>-1</sup> HNO<sub>3</sub> aq.; the  $\Delta E_a$  of CP-Ti had little dependence on the HNO<sub>3</sub> concentration. These results indicate the involvement of two factors; destruction of the titanium oxide layer by F<sup>−</sup> and dissolution of the pure titanium substrate. Titanium substrate etching by decreasing the pH to achieve scale peeling is a promising method for efficient scale removal. The anodic and cathodic polarization behaviors both significantly depend on the HF concentration because of the increased F<sup>−</sup> and H<sup>+</sup> activities; however, HNO<sub>3</sub> addition at the concentrations used in this work has little influence on the anodic parameters. This be-

havior indicates that protons do not eliminate the titanium oxide layer.

## Acknowledgement

We would like to thank Kobe Steel Ltd. for the titanium metal samples and financial support.

## REFERENCES

- 1) J.J. Kelly: *Electrochim. Acta* **24** (1979) 1273–1282.
- 2) D.J. Blackwood, L.M. Peter and D.E. Williams: *Electrochim. Acta* **33** (1988) 1143–1149.
- 3) Y. Ohko, D.A. Tryk, K. Hashimoto and A. Fujishima: *J. Phys. Chem. B* **102** (1998) 2699–2704.
- 4) L. Hong and H. Lin: *Sens. Actuators A Phys.* **232** (2015) 94–98.
- 5) C.F. Ribeiro, K. Cogo-Müller, G.C. Franco, L.R. Silva-Concilio, M.S. Campos, S.D.M. Rode and A.C.C. Neves: *Arch. Oral Biol.* **69** (2016) 33–39.
- 6) W.J. Kroll: *J. Electrochem. Soc.* **78** (1940) 35–47.
- 7) F.S. Wartman, Don H. Baker, J.R. Nettle and V.E. Homme: *J. Electrochem. Soc.* **101** (1954) 507–513.
- 8) R.O. Suzuki, K. Ono and K. Teranuma: *Metall. Mater. Trans., B* **34** (2003) 287–295.
- 9) G.Z. Chen, D.J. Fray and T.W. Farthing: *Nature* **407** (2000) 361–364.
- 10) R. Barnett, K.T. Kilby and D.J. Fray: *Metall. Mater. Trans., B* **40** (2009) 150–157.
- 11) Y. Murakami and K. Sakai: Nippon Steel Technical Report **62** (1994) 1–8.
- 12) M. J. Donachie: *Titanium: A Technical Guide, 2nd Edition*, (ASM International, Materials Park, 2000) pp. 55–63.
- 13) H. Nady, M. M. El-Rabiei and M. Samy: *Egypt. J. Petrol.*
- 14) A.R. Shankar, N.S. Karthiselva and U.K. Mudali: *Surf. Coat. Tech.* **235** (2013) 45–53.
- 15) Z.B. Wang, H.X. Hu, C.B. Liu and Y.G. Zheng: *Electrochim. Acta* **135** (2014) 526–535.
- 16) Z.B. Wang, H.X. Hu and Y.G. Zheng: *Electrochim. Acta* **170** (2015) 300–310.
- 17) E.M.M. Sutter and G.J. Goetz-Grandmont: *Corros. Sci.* **30** (1990) 461–476.
- 18) N.T. Thomas and K. Nobe: *J. Electrochem. Soc.* **117** (1970) 622–626.
- 19) W.E. Hatfield, P.J. Nassiff, T.W. Couch and J.F. Villa: *Inorg. Chem.* **10** (1971) 368–373.
- 20) R. M. Smith and A. E. Martell: *Critical Stability Constants, Inorganic Complexes*, (Plenum Press, New York, 1976).
- 21) H.J. Flitt and D.P. Schweinsberg: *Corros. Sci.* **47** (2005) 2125–2156.

## Appendix

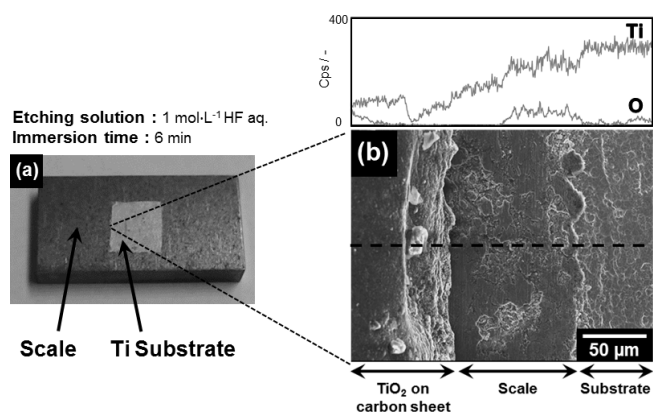


Fig. A1 (a) Photograph of S-Ti after 6 min corrosion with masking using acid-proofed tape in 1 mol·L<sup>-1</sup> HF aq., (b) the SEM images and EDX line profiles of Ti and O with TiO<sub>2</sub> on carbon sheet as a standard (dotted line shows EDX measured area).

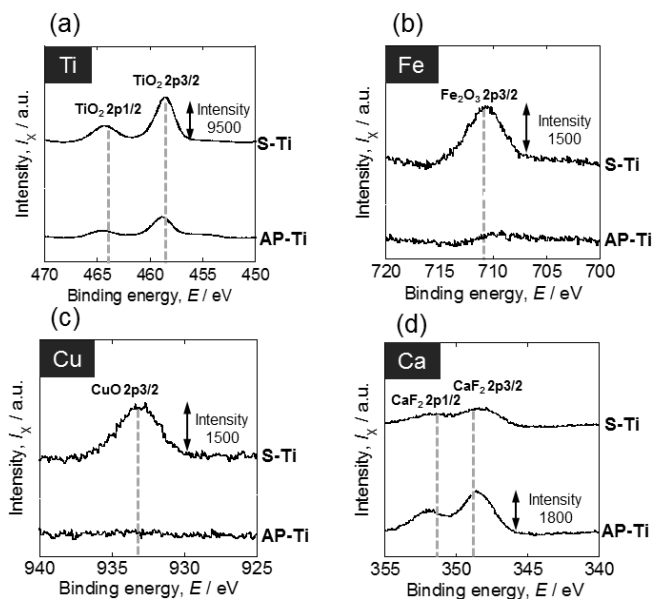


Fig. A2 XPS spectra of S-Ti and AP-Ti of (a) Ti2p, (b) Fe2p, (c) Cu2p, (d) Ca2p.

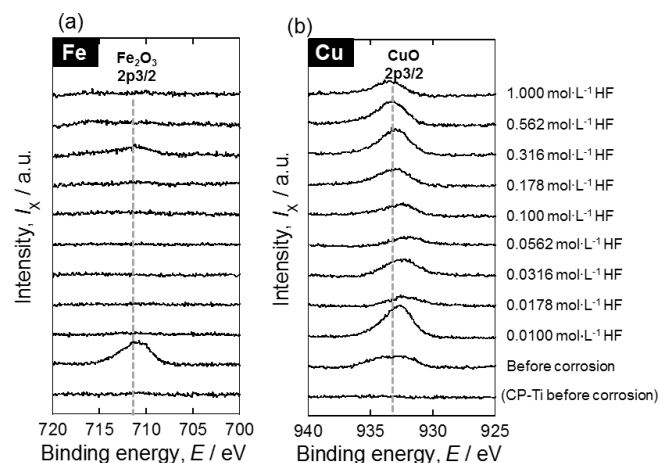


Fig. A3 XPS analysis on S-Ti surface after corrosion in HF system, (a) Fe2p, (b) Cu2p (Immersion time : the 0.1–1 mol·L<sup>-1</sup> HF aq. are 18 min, the others are 180 min).

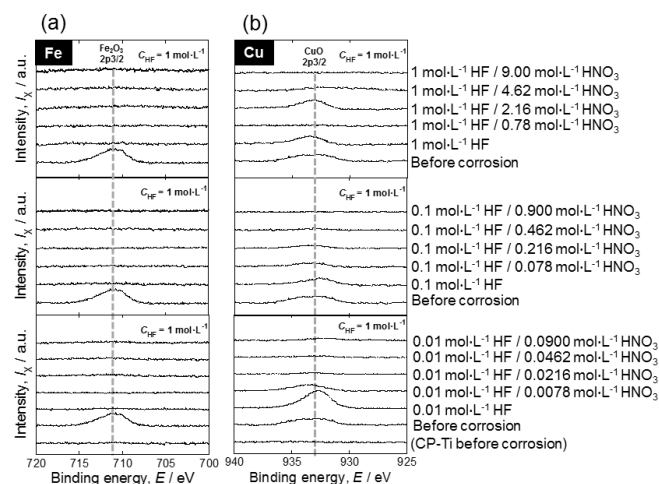


Fig. A4 XPS analysis on S-Ti surface after corrosion in HF-HNO<sub>3</sub> system, (a) Fe2p, (b) Cu2p (Immersion time : the 0.1–1 mol·L<sup>-1</sup> HF aq. are 18 min, the others are 180 min).

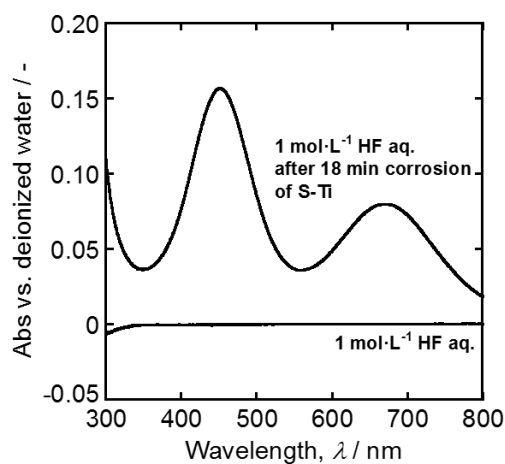


Fig. A5 UV-vis spectra of 1 mol·L<sup>-1</sup> HF aq. and 1 mol·L<sup>-1</sup> HF aq. After 18 min corrosion of S-Ti.

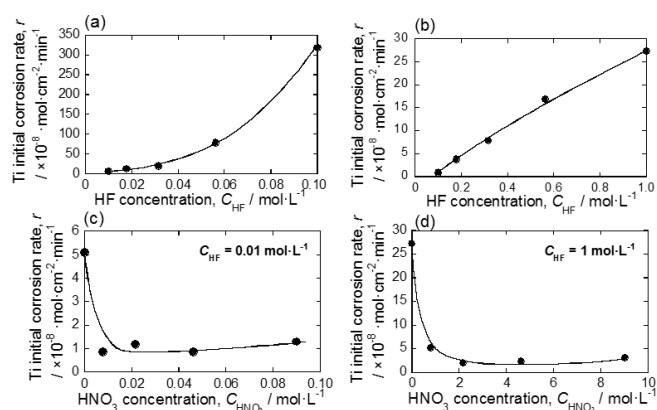


Fig. A7 Calculated Ti initial corrosion rate with S-Ti in (a) 0.01–0.1 mol·L<sup>-1</sup> HF aq., (b) 0.1–1 mol·L<sup>-1</sup> HF aq., (c) 0.01 mol·L<sup>-1</sup> HF aq./0–0.09 mol·L<sup>-1</sup> HNO<sub>3</sub> aq., (d) 1 mol·L<sup>-1</sup> HF aq./0–9 mol·L<sup>-1</sup> HNO<sub>3</sub> aq.

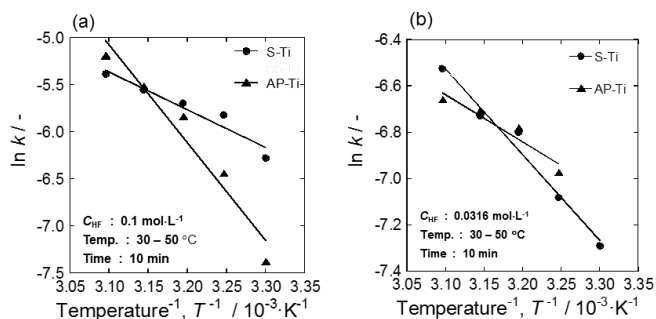


Fig. A6 Arrhenius plots of S-Ti and AP-Ti at a temperature range of 30–50°C in (a) 0.1 mol·L<sup>-1</sup> HF aq., (b) 0.0316 mol·L<sup>-1</sup> HF aq.

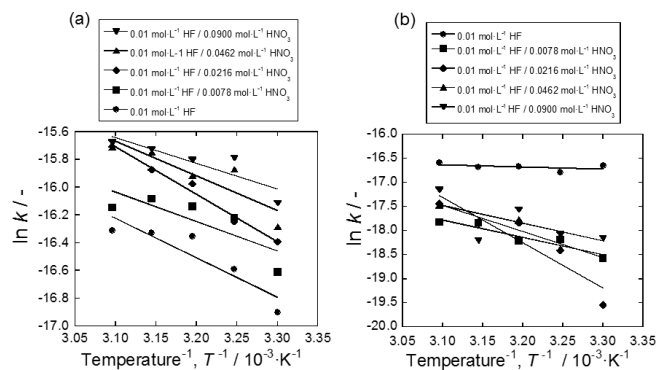


Fig. A8 Arrhenius plots of (a) CP-Ti, (b) S-Ti in 0.01 mol·L<sup>-1</sup> HF aq./0–0.09 mol·L<sup>-1</sup> HNO<sub>3</sub> aq. at a temperature range of 30–50°C.